

The relation of edge confinement to global confinement in ASDEX Upgrade (Axially Symmetric Divertor Experiment)

C. S. Pitcher,^{a)} A. H. Boozer,^{b)} H. Murmann, J. Schweinzer, W. Suttrop, H. Salzmann, the ASDEX Upgrade Team, and NBI Group
Max-Planck-Institut für Plasmaphysik, IPP-EURATOM Association, D-85748 Garching, Germany

(Received 5 December 1996; accepted 3 April 1997)

Experimental evidence is presented from the ASDEX Upgrade (Axially Symmetric Divertor Experiment) tokamak [*Plasma Physics and Controlled Nuclear Fusion Research 1993* (International Atomic Energy Agency, Vienna, 1994), Vol. I, p. 127] of a robust relation between the edge radial pressure gradient and the global confinement of the plasma. This relation transcends the power flowing across flux surfaces near the edge and thus suggests that the usual model of cross-field heat transport, where local gradients increase with increasing local power flow, is not appropriate. © 1997 American Institute of Physics. [S1070-664X(97)02907-8]

I. INTRODUCTION

Cross-field transport at the plasma edge plays a critical role for many aspects of tokamak plasma operation. First, the achievement of H-mode (high-confinement) is thought to be intimately connected to the plasma conditions only centimetres inside of the separatrix.¹ The improved confinement, associated with H-mode, is most noticeable within this narrow region, where a “transport barrier” develops and which is characterized by steep radial gradients of plasma density, temperature and pressure. The improvement in confinement, however, is not limited to the edge region, but clearly extends throughout the entire plasma volume.¹⁻⁴ This is one indication that edge confinement is related to global confinement.

Second, the cross-field transport properties of the plasma edge control the width of the scrape-off layer (SOL) (along with parallel transport rates), and most importantly, the power e -folding width, λ_p , for the parallel flow of power to limiters or divertor plates.^{5,6} For a given plasma heating power, λ_p determines the power density incident on mechanical structures, or alternatively, the radiation density required in dissipative scenarios, such as those presently envisaged for ITER (International Thermonuclear Experimental Reactor).⁷ While it is clear from experiment that λ_p is reduced in H-mode discharges,⁸⁻¹⁰ little else is known at present about how cross-field transport in the edge is related to the global parameters of the plasma. Even empirical scalings are presently scarce.

In this paper we will show experimental evidence from the ASDEX Upgrade (Axially Symmetric Divertor Experiment) tokamak which demonstrates a strong relation between the transport properties of the plasma edge and the global confinement. This not only includes H-modes discharges, but discharges of many types in ASDEX Upgrade. We focus here on the region just inside of the separatrix, in the confined plasma, which in H-mode discharges is referred to as the “transport barrier” or as the “pedestal” region.

We start first in Sec. II with a brief description of ASDEX Upgrade and the boundary diagnostics used in this study. In Sec. III, for reference, we give a commonly used formulation for diffusive cross-field heat flow and in Sec. IV show a consistent experimental example, where gradients at the edge increase approximately in proportion to the cross-field power flow. In Sec. V we give a contrary example for similar plasma conditions, where the gradients at the edge are independent of the power flow. In Sec. VI we suggest a resolution to this apparent contradiction, based on a linkage between edge confinement and global confinement. In Sec. VII we expand the data base to demonstrate that this linkage is a general feature of discharges in ASDEX Upgrade. In Sec. VIII we suggest a non-dimensional scaling so that these results might be compared to other machines. Finally, in Secs. IX and X we discuss the results and conclude.

II. EXPERIMENTAL DETAILS

The ASDEX Upgrade tokamak (AUG), Fig. 1, is a single-null divertor machine, with graphite as the primary first-wall material and neutral beam injection (NBI) heating up to $P_{\text{NBI}} \approx 10$ MW.¹¹ The plasma boundary is extensively diagnosed. Specifically, in this paper we use high resolution electron cyclotron emission (ECE) for T_e profiles,¹² a lithium beam for n_e ¹³ and core and edge Thomson scattering for both n_e and T_e profiles.¹⁴ In the case of the core Thomson system, although the distance between channels is relatively large, ≈ 2 cm, the measurement has high spatial accuracy near the boundary owing to the expanded flux surfaces at the point of measurement, Fig. 1.

Figure 2 gives typical profiles of electron density, temperature and pressure from two identical H-mode discharges with $I_p = 1.0$ MA, $B_t = 2.5$ T, $\bar{n}_e = 8 \times 10^{19} \text{ m}^{-3}$ and $P_{\text{NBI}} = 5.0$ MW. Two discharges are required to obtain both core and edge Thomson measurements, as the same measuring optics are used, requiring a horizontal shift of the system between discharges. All measurements are mapped to the outside midplane with an absolute accuracy of ≈ 1 cm, and a relative accuracy of ≈ 1 mm. Figure 2a includes density measurements from the core and edge Thomson systems and the lithium beam. Figure 2b gives T_e measurements from the

^{a)}Also at MIT Plasma Science and Fusion Center, Cambridge, Massachusetts 02139. Electronic mail: csp@pfc.mit.edu

^{b)}Also at Columbia University, New York, New York 10027.

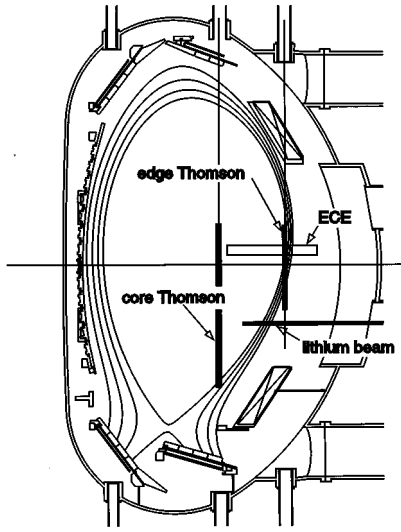


FIG. 1. Poloidal cross-section of ASDEX Upgrade showing the location of boundary diagnostics used in this study.

two Thomson systems. Figure 2c gives the electron pressure p_e profile derived from the two Thomson systems. In general, good agreement is obtained between the various diagnostics, allowing for the ≈ 1 cm absolute positional uncertainty. One exception is the separatrix density as obtained with the core Thomson system, which is approximately a factor of 2 higher than the edge Thomson and the lithium beam, although good agreement with the edge Thomson is obtained in the case of T_e . This discrepancy is ascribed to the difficulty of maintaining the absolute calibration of the Thomson scattering system when shifting the laser beam, the collection optics and the detection system between the edge and core measuring locations.

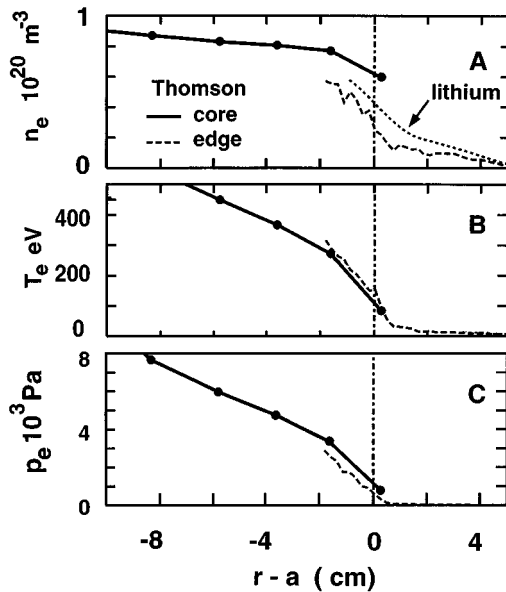


FIG. 2. Profiles of electron density, temperature and pressure in two identical H-mode discharges (7985, 7994) with $I_p=1.0$ MA, $B_t=2.5$ T, $\bar{n}_e=8 \times 10^{19} \text{ m}^{-3}$ and $P_{\text{NBI}}=5.0$ MW. Mapped to the outside mid-plane.

III. CROSS-FIELD TRANSPORT OF POWER

In the absence of ELMs (edge localized modes) or neutral particle sources in the confined plasma, it is commonly assumed in edge plasma work that power moves across field lines in the plasma boundary according to a simple conduction equation,

$$P_{\text{SOL}} = -A_p n_e \chi_{\perp} \frac{dT}{dr}, \quad (1)$$

where P_{SOL} is the power entering the SOL, χ_{\perp} is the anomalous cross-field heat conduction coefficient (ions+electrons, $\chi_{\perp} = \chi_{\perp}^e + \chi_{\perp}^i$) and A_p is the plasma surface area. (In this study we do not measure T_i , and so we simply assume that $T_i = T_e = T$.) According to Eq. (1) therefore, as the power crossing the boundary is increased, other things being equal, the radial temperature gradient should also increase.

In cases where cross-field convection is also present, then it is possible to discuss using a somewhat different equation,

$$P_{\text{SOL}} = -A_p \left(n_e \chi_{\perp} \frac{dT}{dr} + \frac{5}{2} T D_{\perp} \frac{dn}{dr} \right), \quad (2)$$

where D_{\perp} is the cross-field diffusion coefficient (ions + electrons, $D_{\perp} = D_{\perp}^e + D_{\perp}^i$). If we make the simplifying assumption that $D_{\perp} = 2\chi_{\perp}/5$, then we arrive at a convenient equation in terms of electron pressure p_e ,

$$P_{\text{SOL}} = -A_p \chi_{\perp} \frac{dp_e}{dr}. \quad (3)$$

Another approach is to simply use Eq. (3) as an alternative to Eq. (1) for the definition of χ_{\perp} . In any case, the gradients, either of temperature or of pressure, should increase as the cross-field power flow increases (if χ_{\perp} is fixed). It should be noted that we have neglected cross-field power carried by charge-exchange neutrals. This will be a reasonable assumption in cases where neutral particle sources in the confined plasma are small [i.e., Eq. (1)], but less certain in the presence of neutral sources/convection [i.e., Eq. (3)].

From an experimental point of view, one can use Eqs. (1) or (3) along with experimental measurements to derive empirical χ_{\perp} values. We attempt to do this in the next two sections by varying P_{SOL} by two very different methods in otherwise similar hydrogen discharges ($I_p=0.8$ MA, $\bar{n}_e=5.2 \times 10^{19} \text{ m}^{-3}$).

IV. VARYING P_{SOL} USING NBI

In the first experiment (discharges 7808/7810), Fig. 3, P_{SOL} is increased over the Ohmic value using NBI which, according to Eqs. (1) and (3), increases the radial temperature (Fig. 3a) and pressure (Fig. 3b) gradients as determined with the core Thomson system at $r=a-1$ cm. The increase in the gradients is nearly linear at low values of P_{SOL} . The density profile from Thomson scattering and lithium beam in the boundary shows no dependence on P_{SOL} within this data set. P_{SOL} is determined here using $P_{\text{SOL}} = P_{\text{tot}} - P_{\text{rad},Xa}$, where P_{tot} is the total input power and $P_{\text{rad},Xa}$ is the radiated power above the X-point based on bolometer measurements.

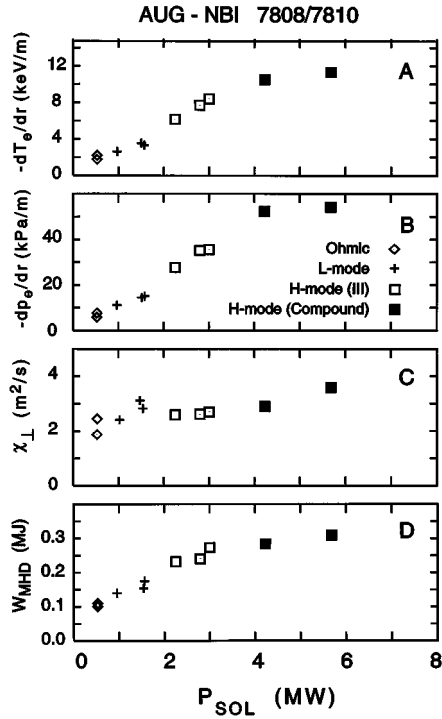


FIG. 3. P_{SOL} scan using varying NBI for two hydrogen discharges (7808, 7810) with $I_p = 0.8$ MA, $B_t = 2.0$ T and $\bar{n}_e = 5.2 \times 10^{19} \text{ m}^{-3}$. Depicted conditions are at $r = a - 1$ cm. (a) Electron temperature gradient. (b) Electron pressure gradient. (c) Derived cross-field heat conduction coefficient according to Eq. (1). (d) Stored energy.

These discharges had relatively low levels of radiated power fraction, i.e., $\approx 30\%$. While this method of determining P_{SOL} is not ideal (e.g., the SOL cannot be resolved), it is the best that can be presently obtained given the limited spatial resolution of the bolometers on ASDEX Upgrade. The data of Figs. 3a and 3b imply an approximately constant value for χ_{\perp} [using Eq. (1)], Fig. 3c.

One should note that these data include Ohmic, L-mode (low confinement) and H-mode discharges, with the H-mode discharges exhibiting Type III and Compound ELMs. Also, the pressure gradient, although rising in a linear fashion for most of the data set appears to saturate at the appearance of Compound ELMs (but not Type III ELMs), at a value which is approximately consistent with the ideal ballooning limit given by,

$$\left| \frac{dp}{dr} \right|_{\text{crit}} = 0.3 \frac{B_t^2 r}{\mu_0 R_0 q^3} \frac{dq}{dr} \quad (4)$$

for simplified geometry (large aspect ratio and circular flux surfaces).¹⁵ In this expression, p is the total pressure (ion + electron), q is the safety factor and R_0 is the major radius. The critical electron pressure gradient at this radial location is calculated (assuming $p_e = p/2$) from magnetic data to be $dp_e/dr_{\text{crit}} \approx -100 \text{ kPa/m}$, which is roughly a factor of ≈ 2 higher than the limit observed in Fig. 3b. Given the experimental error (which is estimated to be $\approx 40\%$), and the error associated with the above simplified expression, the observed pressure gradient limit is consistent. Similar con-

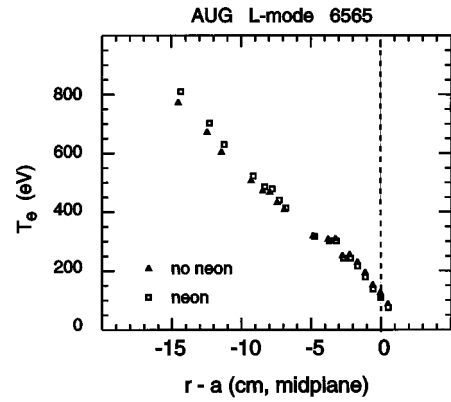


FIG. 4. Electron temperature profile according to ECE in the boundary for a discharge (6565) similar to that of Fig. 3, with and without neon radiation in the plasma periphery. Mapped to the outside mid-plane.

clusions have been made in other studies on Compound and Type I ELMs on ASDEX Upgrade^{16–18} and on other machines.^{1,19–21}

The conditions given in Fig. 3 and at other points in the paper are time-averaged. While the meaning of this may be clear in Ohmic and L-mode discharges, in the case of H-mode discharges with ELMs, it is not immediately obvious what the relation is between the time-averaged gradients and the gradient that initiates a Compound or Type I ELM. Time-resolved measurements on ASDEX Upgrade (not presented here) using ECE and lithium beam^{16–18} and Thomson scattering²² show that the limiting pressure gradient is within $\approx 20\%$ of the time-averaged value. Similar findings have been reported on DIII-D.¹⁹ Considering other uncertainties in these measurements and the approximations inherent in Eq. (4), this difference is negligible.

V. VARYING P_{SOL} USING NEON RADIATION

In the second experiment (discharge 6565, L-mode) the NBI power was maintained constant at $P_{\text{NBI}} = 3$ MW while the level of radiation in the periphery of the confined plasma was varied with neon gas injection. Fig. 4 shows the radial T_e profiles obtained with ECE in this discharge at two times, corresponding to low neon level ($P_{\text{SOL}} \approx 1.8$ MW) and high neon level ($P_{\text{SOL}} \approx 0.8$ MW). Although the resolution of the bolometer system on ASDEX-Upgrade, which is ≈ 5 cm, cannot resolve the SOL, it can identify the neon radiation mantle in the periphery of the confined plasma. This encompasses the volume between $r \approx a - 15$ cm to $r \approx a$, similar to that seen earlier in ASDEX Upgrade^{23,24} and DIII-D.²⁵

The two T_e profiles in Fig. 4 are similar, particularly with respect to the gradients. Closer inspection reveals that the high neon plasma boundary is generally colder close to the separatrix, e.g., the nominal separatrix temperature is ≈ 108 eV in the high neon discharge, compared with ≈ 127 eV in the low neon discharge. This difference, i.e., ≈ 20 eV, is easily resolved by the ECE system, which has a resolution < 1 eV, and is consistent with the factor of ≈ 2.3 difference in P_{SOL} for the two times, assuming that the cross-field power is exhausted along field lines to the divertor according to Spitzer-Härm parallel conductivity.²⁶ Recent studies using

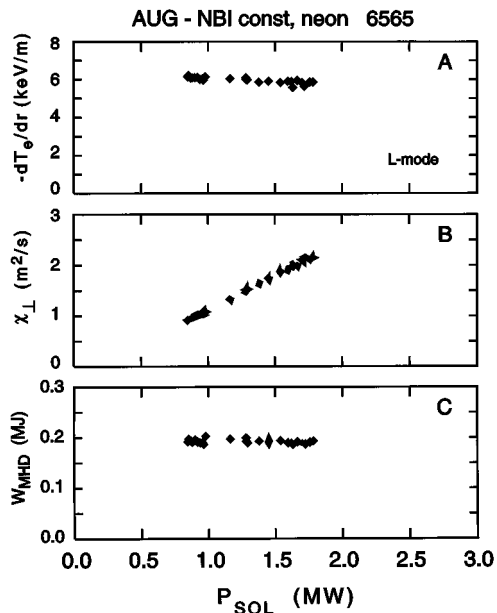


FIG. 5. P_{SOL} scan using varying neon puffing for a hydrogen discharge (6565) with $I_p = 0.8$ MA, $B_t = 2.5$ T and $\bar{n}_e = 5.2 \times 10^{19} \text{ m}^{-3}$. Depicted conditions are at $r = a - 1$ cm. (a) Electron temperature gradient. (b) Derived cross-field heat conduction coefficient according to Eq. (1). (c) Stored energy.

infra-red thermography at the divertor plates in ASDEX Upgrade have shown that the mid-plane separatrix temperature is consistent with Spitzer-Härm conductivity over a wide range of conditions, i.e., parallel power density $\propto T_e^{7/2}$.^{6,22}

The absolute position of the separatrix is not known to better than ± 1 cm, and thus the above quoted temperatures have considerable absolute uncertainty associated with them, although the relative error is expected to be quite small, giving a relatively small error in the determination of the slope. The slope is used along with Eq. (1) to derive χ_{\perp} . Although not shown, the corresponding density profiles from the Thomson scattering systems and the lithium beam are indistinguishable for the two times.

Figure 5 summarizes the results of this experiment, for comparison with Fig. 3, where P_{SOL} was varied using NBI. No change in the radial temperature gradient at $r = a - 1$ cm (Fig. 5a) is measured, implying in this case that $\chi_{\perp} \propto P_{\text{SOL}}$ (Fig. 5b), in contrast to the previous experiment where χ_{\perp} was nearly independent of P_{SOL} for similar plasma conditions.

VI. RELATION TO GLOBAL CONFINEMENT

The results of Figs. 3 and 5, while apparently contradictory, are consistent with the hypothesis that the edge gradient, or effectively, the edge confinement, is correlated with the global confinement. This is demonstrated by Figs. 3d and 5c, which give the global stored energy W_{MHD} for the two experiments. In the case of the first experiment, Fig. 3, the NBI power scan, the stored energy increases approximately as $W_{\text{MHD}} \propto P_{\text{SOL}}^{1/2} \propto P_{\text{tot}}^{1/2}$ (the radiated power fraction is constant) as expected for L-mode and H-mode confinement and, one notes, qualitatively similar to the pressure gradient be-

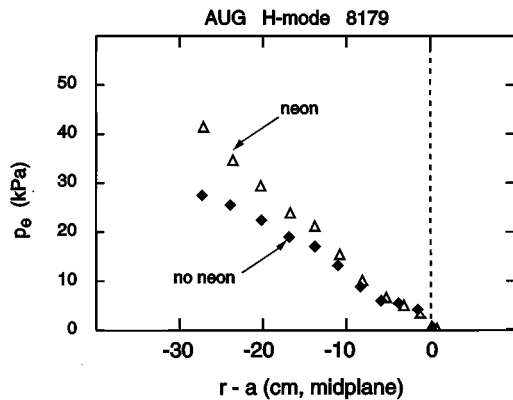


FIG. 6. Electron pressure profile from core Thomson scattering for an H-mode discharge (8179) with $I_p = 1$ MA, $B_t = 2.5$ T, $P_{\text{tot}} = 7.5$ MW, with and without neon puffing. Mapped to the outside mid-plane.

haviour, $dp_e/dr \propto P_{\text{SOL}}$, implying $dp_e/dr \propto W_{\text{MHD}}^2$. The behaviour in the neon experiment is not inconsistent in that the temperature (and pressure) gradient remains constant while the global stored energy remains constant. In this case, while neon radiation greatly increases the radiation losses from the discharge, these losses are primarily in the plasma periphery, and thus have little effect on global confinement. It is, nevertheless, surprising that the edge gradients do not change despite a large variation of radiative loss in the region and the significant change in cross-field plasma power flow.

In Fig. 6 we present another example of the effect of neon, this time in a CDH-mode discharge²⁷ with Type III ELMs (shot 8179, $I_p = 1$ MA, $B_t = 2.5$ T, $P_{\text{tot}} = 7.5$ MW). In this case electron pressure profiles from core Thomson scattering are given. Without neon, $P_{\text{SOL}} \approx 4.2$ MW, compared with $P_{\text{SOL}} \approx 1.6$ MW with neon. The corresponding stored energies are $W_{\text{MHD}} = 0.6$ MJ and $W_{\text{MHD}} = 0.7$ MJ, respectively, i.e., somewhat higher for the case with neon. This is apparent in the figure, where the case with neon has slightly higher electron pressure, although the gradients near the boundary are similar. Despite the factor ≈ 2.6 lower value for P_{SOL} , the case with neon shows a similar radial pressure gradient.

VII. GENERAL RELATION TO GLOBAL CONFINEMENT

The results of the previous section suggest a connection between edge confinement and global confinement. We have investigated whether a general relation holds in other types of discharges, broadening the range of discharge parameters to include $0.6 \text{ MA} < I_p < 1.2 \text{ MA}$, $1.5 \text{ T} < B_t < 3.0 \text{ T}$, $2 \times 10^{19} \text{ m}^{-3} < \bar{n}_e < 1.2 \times 10^{20} \text{ m}^{-3}$, $0.2 \text{ MW} < P_{\text{SOL}} < 6.0 \text{ MW}$, hydrogen/deuterium, fresh/old boronizations, impurity gas puffing and $0.2 < P_{\text{SOL}}/P_{\text{tot}} < 0.9$ — basically all diagnosed and stable discharges between shot 7730 and shot 8235, performed in the spring of 1996. Only steady state conditions were used, which is defined as having constant conditions over periods of greater than 0.5 s. Altogether, 182 separate time-slices result from this selection process.

Figure 7 gives the edge electron pressure gradient as determined by the core Thomson scattering system in the

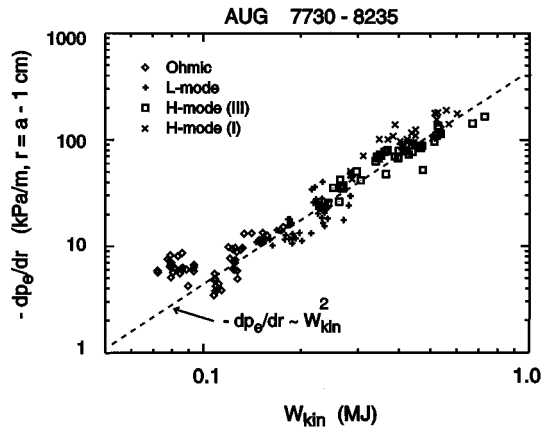


FIG. 7. A general relation between the electron pressure gradient at the boundary ($r = a - 1$ cm) and the stored energy W_{kin} , both from core Thomson scattering. A large range of discharge conditions is included (see the text).

region $r - a = -2$ cm to $r = a$ as a function of discharge stored kinetic energy W_{kin} , also determined by the Thomson system (we assume $T_i = T_e$). (W_{kin} is used here rather than W_{MHD} , since the latter is inaccurate for the low current Ohmic discharges included in this data set.) Despite the very large range of conditions included, a strong correlation between the edge gradient and the global stored energy is obtained, with an identical scaling as found in the previous sections, $dp_e/dr \propto W^2$. This result indicates that as the stored energy is increased, the edge pressure gradient rises faster than the average gradient of the discharge. This is apparent in the pressure profile of Fig. 2c, which illustrates for this H-mode discharge the confinement barrier in the region $r - a = -2$ cm to $r = a$ in a discharge with relatively high stored energy, $W_{\text{MHD}} \approx 0.46$ MJ, and relatively high edge pressure gradient $dp_e/dr \approx -140$ kPa/m. The pressure gradient near the separatrix is larger than the average.

While the data of Fig. 7 was obtained with strictly Ohmic or neutral beam heating, a limited number of ICRH heated discharges show an identical scaling, but are not included here. In addition, no clear dependence on discharge density alone could be detected in the data. These two points argue that the observed scaling for NBI discharges is not related to changes in the neutral beam deposition profile.

One group of data points appears to stand-out from the general scaling in Fig. 7. These are Ohmic discharges with $W < 0.1$ MJ and low plasma current, $I_p = 0.6$ MA. In the next section we present the same data using dimensionless quantities, and in this case these “rogue” points coalesce with the others.

VIII. NON-DIMENSIONAL RELATION

Given the large range of currents and fields included in Fig. 7, the relation $dp_e/dr \propto W_{\text{MHD}}^2$ is perhaps unsatisfying from a dimensional point of view. In Fig. 8 we normalize the data of Fig. 7 using the critical (electron) pressure gradient $0.5dp/dr_{\text{crit}}$ from Eq. (4) and the internal energy stored in the poloidal field, $W_{\text{pol}} \propto I_i^2$, where I_i is the internal induc-

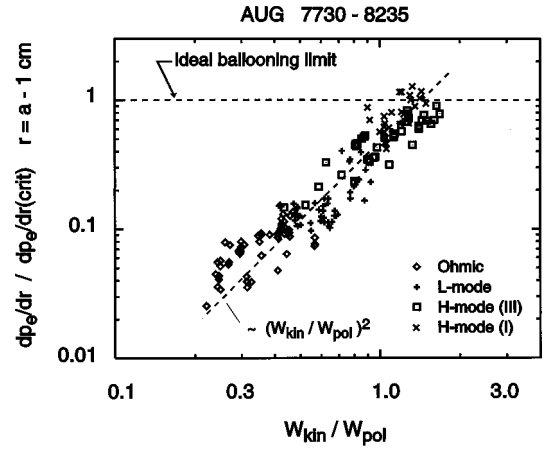


FIG. 8. Reduced data from Fig. 7. The electron pressure gradient is normalized by half of the critical pressure gradient given by Eq. (4). The stored energy W_{kin} is normalized by the internal energy stored in the poloidal field, $W_{\text{pol}} \propto I_i^2$.

tance of the discharge. The horizontal scale is approximately the poloidal beta, β_p (dp/dr_{crit} is calculated using the q profile, as determined from a magnetics code).

Figure 8 serves two important purposes. First, since we can't at present explain the reason for the $dp_e/dr \propto W^2$ scaling in the primary data, it is important to demonstrate that normalized quantities also give a reasonable fit to the data. This allows comparisons with other machines with different sizes, fields, currents and powers. At the present time, however, it is not clear to us which form of normalization is most appropriate for this data. The fact that the normalization brings the “rogue” low current Ohmic discharges into agreement with the other discharges is perhaps some indication that this type of normalization is appropriate. Nevertheless, Fig. 8 is simply one possible means of reducing the data.

Second, Fig. 8 illustrates the continuous increase in edge pressure gradient from Ohmic discharges, through to L-mode, H-mode with Type III ELMs and finally to H-mode discharges with Type I ELMs (for convenience, Compound ELMs have been excluded in this analysis). Type I ELMs tend to group together in the vicinity of the ideal ballooning limit, $dp_e/dr \approx 0.5dp/dr_{\text{crit}}$, at high values of normalized stored energy. Similar findings have been reported in Refs. 1 and 16–21.

IX. DISCUSSION

The primary result of this study is that a robust relation exists in ASDEX Upgrade between the edge gradients (or edge confinement) and the global confinement. This is manifest by the simple relation, $dp_e/dr \propto W^2$, or in other words, the pressure gradient at the boundary increases more rapidly than the global pressure gradient ($\approx W/a$). While this is most noticeable in H-mode discharges, where the “confinement barrier” becomes readily apparent (Fig. 2), it is also true in all other regimes so far investigated. This includes a large range of currents, fields, densities and radiated power fractions.

It is important to realize that although we have discussed the experimental results primarily in terms of pressure, the observations are also consistent with a strong relation between the edge temperature gradient and global temperature gradient (i.e., $dT_e/dr \propto \langle T_e \rangle^2$). Our bias has been towards pressure simply because the limiting gradient at the edge is consistent with ideal ballooning, rather than a temperature gradient limit.

The fact that the pressure gradient at the boundary appears to depend only on the total stored energy, and not the cross-field power flowing through the region, argues against our standard notion of heat flow at the boundary, i.e., Eqs. (1) and (3). Instead, the boundary gradient is simply related to the global gradient, and the power flowing across the field lines appears irrelevant. This picture, while perhaps surprising, is consistent with a global picture of transport as suggested by Cordey *et al.*⁴ and Gentle *et al.*^{28,29} and other references there mentioned. The hypothesis is that the cross-field transport arises due to plasma turbulence which is linked in the radial direction by the toroidal geometry inherent in tokamaks.³⁰

Aside from the experimental data presented here, there are now several experimental results which argue for this global picture of cross-field transport. These include transport studies of the L to H transition, where several tokamaks have found that the confinement improvement in the core region follows only milliseconds after the development of the edge transport barrier, i.e., in a time-scale much faster than the diffusive time based on equilibrium transport coefficients.^{4,31,32} Similarly, cold gas puffs^{28,29} and sawtooth heat pulses³³ both propagate much faster in the radial direction than equilibrium transport would suggest. Confinement degradation on the Wendelstein stellarator on the application of ECRH occurs before changes in local parameters.³⁴ Transport studies in L-mode discharges in TFTR (Tokamak Fusion Test Reactor)³⁵ and JET (Joint European Torus)³⁶ indicate a ‘‘Bohm-like’’ scaling, which only arises when the radial cell size for fluctuations is independent of the Larmor radius and an appreciable fraction of the minor radius.

Our results, in which the location of the power sink is varied using neon puffing, are the compliment of earlier studies on other machines where the radial location of the power source was varied, with little resulting change in the temperature profile (see review by Wagner and Stroth³⁷). This tendency for the profile shape, particularly in the plasma periphery, to be independent of heating location is known as ‘‘profile consistency’’³⁸ or more recently, ‘‘profile resiliency.’’³⁹ Evidently, the edge plasma profile just inside the separatrix is similarly resilient. It should be noted, however, that there are counter examples to profile resiliency, albeit for the core region, where localized off-axis heating has resulted in profile shape changes.^{37,40}

There is an alternative to the above global model which is also consistent with the present observations on ASDEX Upgrade and the earlier ones on other machines. This states that the plasma is marginally stable against transport across most of the plasma cross-section, resulting in transport coefficients which are highly non-linearly dependent on the local quantities.^{37,41,42} For example, if the local χ_{\perp} has a very

strong dependence on the local temperature or the temperature gradient, any attempt to change the temperature profile by either locally heating or locally cooling would result in little change to the profile anywhere. Further, in such a scenario, local perturbations should propagate faster in the radial direction than expected from equilibrium transport coefficients, also as is often observed. Based on the present observations, we cannot choose between either the global model or the local model.

The results presented in this paper have focussed on the edge plasma just inside the separatrix, and not the region outside of the separatrix, i.e., the SOL. Cross-field transport in the latter determines the parallel power width in the SOL, λ_p , which is a critical parameter for the divertor. While the cross-field power flux is undoubtedly continuous across the separatrix, this is not necessarily true of the gradients of density, temperature and pressure. Thus, the pressure gradient scaling observed here may not be applicable to the SOL. Clearly, detailed studies similar to the present are required in the SOL. Some have already indicated a link between λ_p and the global confinement.^{8–10}

X. CONCLUSIONS

We have presented experimental evidence from the ASDEX Upgrade tokamak of a robust relation between the edge radial pressure gradient and the global confinement of the plasma. This relation transcends the power flowing across flux surfaces near the edge and thus suggests that the usual model of cross-field heat transport, where local gradients increase with increasing local power flow, is not appropriate. These results are consistent with data from other tokamaks which suggest either a global picture of cross-field transport or a local model, where transport is dependent on local quantities in a highly non-linear fashion.

ACKNOWLEDGMENTS

C. S. Pitcher is thankful for personal support during this study from the Max-Planck-Institut für Plasmaphysik and the Canadian Fusion Fuels Technology Project. This work is also supported by U.S. Department of Energy Contract No. DE-AC02-78ET51013.

¹R. J. Groebner, *Phys. Fluids B* **5**, 2343 (1993).

²G. Becker, D. Campbell, A. Eberhagen and the ASDEX Team, *Nucl. Fusion* **23**, 1293 (1983).

³S. M. Kaye, M. G. Bell, K. Bol, and the PDX Team, *J. Nucl. Mat.* **121**, 115 (1984).

⁴J. G. Cordey, D. G. Muir, V. V. Parail, G. Vayakis, S. Ali-Arshad, D. V. Bartlett, D. J. Campbell, A. L. Colton, A. E. Costley, R. D. Gill, A. Loarte, S. V. Neudachin, L. Porte, A. C. C. Sips, E. M. Springmann, P. M. Stuberfeld, A. Taroni, K. Thomsen, and M. G. Von Hellermann, *Nucl. Fusion* **35**, 505 (1995).

⁵F. Wagner and K. Lackner, in *Physics of Plasma-Wall Interactions in Controlled Fusion*, edited by D. E. Post and R. Behrisch, NATO ASI Series (Plenum, New York, 1986), p. 931.

⁶C. S. Pitcher and P. C. Stangeby, *Plasma Phys. Controlled Fusion* (in press, 1997).

⁷J. Janeschitz, K. Borrass, G. Federici, Y. Igitkhanov, A. Kukushkin, H. D. Pacher, G. W. Pacher, and M. Sugihara, *J. Nucl. Mat.* **220–222**, 73 (1995).

⁸D. H. Hill, T. Petrie, M. Ali Mahdavi, L. Lao, and W. Howl, *Nucl. Fusion* **28**, 902 (1988).

⁹ASDEX Team, *Nucl. Fusion* **29**, 1959 (1989).

- ¹⁰B. LaBombard, J. A. Goetz, I. Hutchinson, D. Jablonski, J. Kesner, C. Kurz, B. Lipschultz, G. M. McCracken, A. Niemczewski, J. Terry, and the C-Mod Team, *J. Nucl. Mat. Proceedings of the 12th PSI Conference* (in press, 1997).
- ¹¹W. Köppendörfer, C. Andelfinger, M. Ballico, and the ASDEX Upgrade and NBI Teams, *Proceedings of the 14th Conference Proceedings on Plasma Physics and Controlled Nuclear Fusion Research, 1992, Würzburg* (International Atomic Energy Agency, Vienna, 1993), Paper IAEA-CN-56/A-2-3, Vol. I, p. 127.
- ¹²N. A. Salmon, *Int. J. IR and Millimeter Waves* **15**, 53 (1994).
- ¹³J. Schweinzer, S. Fiedler, O. Gehre, G. Haas, J. Neuhauser, D. Wutte, H. P. Winter, ASDEX Upgrade, NBI, ICRH, ECRH Teams, *European Physical Society Conference on Plasma Physics and Controlled Fusion*, Bournemouth (European Physical Society, Petit-Lancy, 1995), Vol. III, p. 253.
- ¹⁴H. Murmann, S. G. ötsch, H. Röhr, H. Salzmann, and K. H. Steuer, *Rev. Sci. Instrum.* **63**, 4941 (1992).
- ¹⁵J. W. Connor, R. J. Hastie, and J. B. Taylor, *Phys. Rev. Lett.* **40**, 396 (1978).
- ¹⁶W. Suttrop, K. Schönmann, J. Schweinzer, H. Zohm, M. Alexander, H. Reimerdes, ASDEX Upgrade Team, NBI group and ICRH group, *European Physical Society Conference on Plasma Physics and Controlled Fusion*, Bournemouth (European Physical Society, Petit-Lancy, 1995) Vol. III, p. 237.
- ¹⁷W. Suttrop, K. Büchl, H. J. de Blank, J. Schweinzer, H. Zohm, and the ASDEX Upgrade and NBI Teams, *Plasma Phys. Control Fusion* **38**, 1407 (1996).
- ¹⁸W. Suttrop, H. J. de Blank, G. Haas, H. Murmann, O. Gehre, H. Reimerdes, F. Rytter, H. Salzmann, J. Schweinzer, J. Stober, H. Zohm, ASDEX Upgrade Team, NBI Team, and ICRH Team, *European Physical Society Conference on Plasma Physics and Controlled Fusion*, Kiev (European Physical Society, Petit-Lancy, 1996).
- ¹⁹P. Gohil, M. Ali Mahdavi, L. Lao, K. H. Burrell, M. S. Chu, J. C. DeBoo, C. L. Hsieh, N. Ohya, R. T. Snider, R. D. Stambaugh, and R. E. Stockdale, *Phys. Rev. Lett.* **61**, 1603 (1988).
- ²⁰H. Zohm, T. H. Osborne, K. H. Burrell, M. S. Chu, E. J. Doyle, P. Gohil, D. N. Hill, L. L. Lao, A. W. Leonard, T. S. Taylor, and A. D. Turnbull, *Nucl. Fusion* **35**, 543 (1995).
- ²¹H. Zohm, *Plasma Phys. Controlled Fusion* **38**, 105 (1996).
- ²²C. S. Pitcher, A. Herrmann, H. Murmann, H. Reimerdes, J. Schwinzer, W. Suttrop, H. Salzmann and the ASDEX Upgrade Team and NBI Group, to appear in *Plasma Physics Controlled Fusion* (in press, 1997).
- ²³A. Kallenbach and the ASDEX Upgrade and NBI Teams, *Nucl. Fusion* **35**, 1231 (1995).
- ²⁴R. Dux, A. Kallenbach, M. Bessenrodt-Weberpals, K. Behringer, H.S. Bosch, J. C. Fuchs, O. Gehre, F. Mast, W. Poschenrieder, H. Murmann, H. Murmann, H. Salzmann, J. Schweinzer, W. Suttrop, and the ASDEX Upgrade Team and the NI Team, *Plasma Physics Controlled Fusion* **38**, 989 (1996).
- ²⁵D. N. Hill, S. L. Allen, N. H. Brooks, and the DIII-D Team, *Proceedings of the 15th Conference on Plasma Physics and Controlled Nuclear Fusion Research*, 1994, Seville (International Atomic Energy Agency, Vienna, 1995), Paper IAEA-CN-60/A-4-I-2, Vol. I, p. 499.
- ²⁶L. Spitzer and R. Härm, *Phys. Rev.* **89**, 977 (1953).
- ²⁷J. Neuhauser and the ASDEX Upgrade Team and NBI Team, *Plasma Phys. Controlled Fusion* **37**, A37 (1995).
- ²⁸K. W. Gentle, G. Cima, H. Gasquet, G. A. Hallock, P. E. Phillipps, W. L. Rowan and C. Watts, *Phys. Scr.* **52**, 411 (1995).
- ²⁹K. W. Gentle, R. V. Bravenec, G. Cima, H. Gasquet, G. A. Hallock, P. E. Phillipps, D. W. Ross, W. L. Rowan, A. J. Wootton, T. P. Crowley, J. Heard, A. Ouroua, P. M. Schoch, and C. Watts, *Phys. Plasmas* **2**, 2292 (1995).
- ³⁰J. W. Connor, R. J. Hastie and J. B. Taylor, *Proc. R. Soc. Lond. Ser. A* **365**, 1 (1979).
- ³¹G. Becker and H. Murmann, *Nucl. Fusion* **28**, 2179 (1988).
- ³²T. K. Kurki-Suonio, K. H. Burrell, R. J. Groebner, R. Philippona, and C. L. Rettig, *Nucl. Fusion* **33**, 301 (1993).
- ³³E. D. Fredrickson, K. McGuire, A. Cavallo, R. Budny, A. Janos, D. Monticello, Y. Nagayama, W. Park, G. Taylor, and M. C. Zarnstorff, *Phys. Rev. Lett.* **65**, 2869 (1990).
- ³⁴U. Stroth, in *Local Transport Studies in Fusion Plasmas* (Societa Italiana di Fisica, Bologna, 1994), p. 161.
- ³⁵F. W. Perkins, C. W. Barnes, D. W. Johnson, S. D. Scott, M. C. Zarnstorff, M. G. Bell, R. E. Bell, C. E. Bush, B. Grek, K. W. Hill, D. K. Mansfield, H. Park, A. T. Ramsey, J. Schivell, B. C. Stratton, and E. Synakowski, *Phys. Fluids B* **5**, 477 (1993).
- ³⁶J. P. Christiansen, P. M. Stubberfield, J. G. Cordey, C. Gormezano, C. W. Gowers, J. O'Rourke, D. Stork, A. Taroni, and C. D. Challis, *Nucl. Fusion* **33**, 863 (1993).
- ³⁷F. Wagner and U. Stroth, *Plasma Physics Controlled Fusion* **35**, 1321 (1993).
- ³⁸B. Coppi, *Comments Plasma Phys. Controlled Fusion* **5**, 261 (1980).
- ³⁹R. J. Goldston, Y. Takase, D. C. McCune, M. G. Bell, M. Bitter, C. E. Bush, P. H. Diamond, P. C. Efthimion, E. D. Fredrickson, B. Grek, H. Hendel, K. W. Hill, D. W. Johnson, D. Mansfield, K. McGuire, E. Nieschmidt, H. Park, M. H. Redi, J. Schivell, S. Sesnic, and G. Taylor, *European Physical Society Conference on Plasma Physics and Controlled Fusion, Madrid, 1987* (European Physical Society, Petit-Lancy, 1988), Vol. IID, Part 1, p. 140.
- ⁴⁰J. G. Cordey and JET Team, *Proceedings of the 14th Conference on Plasma Physics and Controlled Nuclear Fusion Research, 1992, Würzburg* (International Atomic Energy Agency, Vienna, 1993), Paper IAEA-CN-56/D-3-4, Vol. II, p. 161.
- ⁴¹W. K. Gentle, B. Richards, M. E. Austin, R. V. Bravenec, D. L. Brower, R. F. Gandy, W. L. Li, P. E. Phillips, D. W. Ross, W. L. Rowan, P. M. Schoch, P. M. Valanju, and A. J. Wootton, *Phys. Rev. Lett.* **68**, 2444 (1992).
- ⁴²M. Kotschenreuther, W. Dorland, Q. P. Liu, G. W. Hammett, M. A. Beer, S. A. Smith, A. Bondeson, and S. C. Cowley, *Proceedings of the 16th Conference on Plasma Physics and Controlled Nuclear Fusion Research, 1996, Montreal* (International Atomic Energy Agency, Vienna, 1997), IAEA-CN-64/D1-5, in press.